



HAL
open science

Preoperative assessment of idiopathic scoliosis in adolescent and young adult with three-dimensional T2-weighted spin-echo MRI

T. Duchaussoy, M. Lacoste, L. Norberciak, J. Decaudain, S. Verclytte, J.-F. Budzik

► To cite this version:

T. Duchaussoy, M. Lacoste, L. Norberciak, J. Decaudain, S. Verclytte, et al.. Preoperative assessment of idiopathic scoliosis in adolescent and young adult with three-dimensional T2-weighted spin-echo MRI. *Diagnostic and Interventional Imaging*, 2019, 100, pp.371 - 379. 10.1016/j.diii.2019.01.010 . hal-03486293

HAL Id: hal-03486293

<https://hal.science/hal-03486293v1>

Submitted on 20 Dec 2021

HAL is a multi-disciplinary open access archive for the deposit and dissemination of scientific research documents, whether they are published or not. The documents may come from teaching and research institutions in France or abroad, or from public or private research centers.

L'archive ouverte pluridisciplinaire **HAL**, est destinée au dépôt et à la diffusion de documents scientifiques de niveau recherche, publiés ou non, émanant des établissements d'enseignement et de recherche français ou étrangers, des laboratoires publics ou privés.



Distributed under a Creative Commons Attribution - NonCommercial 4.0 International License

Preoperative assessment of idiopathic scoliosis in adolescent and young adult with three- dimensional T2-weighted spin-echo MRI

Preoperative MRI of adolescent idiopathic scoliosis

Thomas Duchaussoy¹, Marion Lacoste¹, Laurène Norberciak², Julien Decaudain^{3,4},
Sébastien Verclytte^{1,4}, Jean-François Budzik^{1,4,5*}

1. Lille Catholic Hospitals, Imaging Department, 59000 Lille, France
2. Lille Catholic Hospitals, Clinical Research and Innovation Department, 59000 Lille, France
3. Lille Catholic Hospitals, Orthopedic Surgery Department, 59000 Lille, France
4. Lille Catholic University, 59000 Lille, France
5. PMOI Physiopathology of Inflammatory Bone Diseases, EA 4490, 59000 Lille, France

Corresponding author: *JF Budzik

Budzik.Jean-Francois@ghicl.net

Abstract

Purpose. To compare tridimensional (3D) T2-weighted spin echo MRI and CT for minimal pedicle width measurements in the preoperative assessment of adolescent idiopathic scoliosis (AIS) in adolescent and young patients.

Materials and methods. A total of 22 adolescents/young patients suffering from AIS were retrospectively included. There were 18 females and 4 males with a mean age of 15.3 ± 2.3 (SD) years (range: 11-21 years). Preoperative lumbar spine MRI and CT examinations of the 22 patients were reviewed by two independent readers who measured the minimal width of 259 pedicles. Inter-reader agreement for CT and MRI was assessed using intra-class correlation coefficients (ICC). Intra-reader agreement and relative differences in measurements between MRI and CT were also assessed for each reader.

Results. Inter-reader agreement was excellent ($ICC \geq 0.8$) for both CT and MRI. Relative differences in measurements between CT and MRI was 10.3% for reader 1 and 9.4% for reader 2.

Conclusion. 3D T2-weighted spin-echo MRI underestimates minimal pedicle width by about 10% compared to CT. 3D T2-weighted MRI appears as a valuable alternative to CT for preoperative measurements of vertebral pedicles in AIS.

Keywords: Adolescent idiopathic scoliosis (AIS); Scoliosis; Magnetic resonance imaging; Multidetector computed tomography; Radiation protection.

Abbreviations

AIS	Adolescent idiopathic scoliosis
MPW	Minimal pedicle width
PACS	Picture archiving and communication system

Introduction

Adolescent idiopathic scoliosis (AIS) affects 0.5 to 5.2% of children and teenagers between 10- and 18-year-old (1). Management of AIS consists in observation for AIS with mild curves, brace treatment for moderate curves and surgery for curves $\geq 50^\circ$ (1). The goal of surgical treatment is to reduce spine deformity and prevent further progression (2). It relies on thoracolumbar arthrodesis with posterior instrumentation (2). Screws are inserted in vertebral pedicles at the lumbar level or the thoracolumbar junction, whereas rods are fixed on thoracic posterior arches with hooks. Large diameter screws are less prone to future breakage than thin diameter screws, but their insertion increases the risk of intraoperative cortical breach and subsequently injury to adjacent structures (3–5). The reported rate of cortical perforation varies widely from 1.2 to 65% (5), and serious complications such as epidural hematoma, nerve root injury with neurological deficit, vascular lesions such as direct aortic trauma or false aneurysm, and lung perforation have been reported (5).

For the surgeon, the most relevant information in the preoperative work-up is the minimal pedicle width (MPW) (i.e., the minimal inner cross-sectional diameter of the pedicle) (3). The MPW is the distance separating the medial cortical bone from the lateral cortical bone. As these measures involve cortical bone, CT has been thoroughly used and is still widely used (3,5,6–11). However, because of radiation concerns, CT should no longer be used for the preoperative assessment of AIS and be replaced by magnetic resonance imaging (MRI) (7).

When surgery is considered as a treatment option for AIS, it is performed during late adolescence. Indeed, skeletal maturity has to reach a certain stage to avoid the “crankshaft phenomenon”. This refers to progression and rotation of the scoliosis due to continued growth of the anterior part of spinal elements after posterior spinal fusion, which might occur in skeletally immature patients (12). Dose reduction is a constant concern in AIS imaging (13). MRI is the imaging modality of choice in this context because it does not use radiation and is commonly used in spine imaging. As technique improves, evidence has accumulated validating MRI as an alternative to CT (14). However, the use of MRI in the preoperative assessment of AIS has not received special attention so far.

The purpose of this study was to compare tridimensional (3D) T2-weighted spin-echo MRI with CT for minimal pedicle width measurements in the preoperative assessment of AIS in adolescent and young patients.

Materials and methods

This retrospective monocentric study received local ethics committee approval.

Patients

We retrospectively analysed the files of all consecutive patients with AIS who were surgically treated in our institution between June 2015 and October 2017. Patients suffering from AIS were included whatever the morphology or topography of their scoliosis. The initial search retrieved a total of 29 patients with AIS who underwent surgery during this period. Patients were further included when they had undergone preoperative MRI of the spine and lumbar CT examinations at our institution less than 2 weeks of each other. Potential participants were excluded from the study population if they did not want their images used for research purposes. The study flow chart is shown in Figure 1. The database search identified 26 patients who fulfilled the study inclusion criteria. Four patients were further excluded as they declined the use of their data for research purposes. The study population ultimately included 22 patients. There were 18 females and 4 males with a mean age of 15.3 ± 2.3 (SD) years (range: 11-21 years).

MRI protocol

MRI studies were performed either on a 1.5T MR Discovery[®] 450W (General Electric Healthcare) (17/22 patients; 77%) or a 3T Discovery[®] MR750w (General Electric Healthcare) (5/22 patients; 23%). We used a 40-channel phased-array spine coil that was integrated in the examination bed. A 3D fast spin-echo T2-weighted sequence was used to cover the whole lumbar spine. MRI parameters are described in Table 1.

CT protocol

CT was performed from T12 to S1 using a Lightspeed[®] VCT XT (General Electric Healthcare) or a Somatom[®] Definition Edge (Siemens Healthineers) unit. On both CT machines, a standard pediatric spine protocol was used. Imaging parameters were as follows: 120 kVp tube voltage, mA depending on topogram-based dose modulation algorithm; 1mm slice thickness; pitch, 0.65; rotation time, 1 s. Images were reconstructed at 0.6 mm-slice thickness using a bone kernel.

Data analysis

All MRI and CT images were anonymized on the PACS (Carestream Healthcare) and reviewed by the study coordinator (J.F.B.) to ensure that they were exempt from visible artifacts that could impede their interpretation. Then they were independently reviewed by two musculoskeletal imaging residents (T.D., 5th year resident, as reader 1, and M.L., 5th year resident as reader 2). CT and MRI examinations were analyzed on the PACS viewer with multiplanar reconstruction in a random order and separately, on separate sessions at least one week apart. For each vertebral pedicle from T12 to S1, and for each imaging technique, the radiologists reconstructed images in the coronal plane of the pedicles. Then, they measured the distance separating the medial cortical bone from the lateral cortical bone, corresponding to MPW using electronic calipers (Figs. 2, 3).

Statistical analysis

Statistical analysis was performed using the R software (version 3.4). For each reader, differences in MPW measurements between MRI and CT were initially assessed by computing the intra-class correlation coefficient (ICC) and its 95% confidence interval (CI) for each pedicle. Indeed, because of repeated measures for each patient (12 pedicles), the correlation between the pedicles did not allow calculating a global ICC. The same calculations were performed to assess the inter-observer agreement for MPW measurements on MRI (MRI reader 1 vs. 2), and then CT (CT reader 1 vs. 2). Irr package (R software) was used taking into account a model with two random factors, with estimates of agreement on the raw data. The agreement was considered very good if the ICC was greater than 0.8 strictly, good if the ICC was between 0.61 and 0.8, moderate if the ICC was between 0.6 and 0.41, bad otherwise. The MRI-CT relative difference for reader, and CT-CT relative difference between readers were calculated for each patient. More precisely, for each reader, MRI-CT relative difference was $(\text{MRI} - \text{CT}) / \text{CT}$, and CT-CT difference between readers was $(\text{CT reader 2} - \text{CT reader 1}) / \text{CT reader 1}$. Quantitative variables were expressed as means, standard deviations (SD), and 95% CI.

Results

All imaging examinations were deemed technically adequate for the purpose of this study. For each patient, right and left pedicles were measured from T12 to S1, apart from five

T12 pedicles that were incompletely covered during image acquisition, yielding 259 analyzed pedicles. No neurological or congenital vertebral abnormalities were found. Table 1 shows the distribution of the CT measurements made by reader 1. Briefly, 257/259 measures (99.2%) were < 10mm, and 221/259 (85.3%) measures were < 7mm. Mean CT radiation dose was 300 ± 172 (SD) mGy.cm (range: 128-472 mGy.cm).

Regarding CT-MRI agreement, ICC was > 0.8 for all individual pedicles except L5D for reader 1 (ICC=0.76) (Table 2). Consequently, the agreement between MRI and CT measurements for a given reader was considered excellent.

Regarding inter-observer agreement, ICC was > 0.8 for all individual pedicles for both MRI and CT, except for L4G MRI measurements (ICC=0.8) (Table 2). Consequently, inter-observer agreement was considered excellent for both protocols.

Mean MRI-CT relative difference was -10.3 ± 18.6 (SD) % for reader 1 (95% CI: -12.6%; -8.1%), and -9.4 ± 19.5 (SD) % for reader 2 (95% CI: -11.8%; -7%) (Fig. 4). Mean CT-CT difference between readers was -5.1 ± 11.3 (SD) % (95% CI: -6.5%; -3.7%).

Discussion

According to our results, MPW measurements on 3D T2-weighted spin echo MRI sequences were underestimated by approximately 10% by comparison with CT. However, the error margin for CT measurements was approximately 5%. It is noticeable that the 10% underestimation of MPW measurement obtained with MRI in our study was determined relative to CT measurements. CT can be considered as the standard of reference but to our knowledge, the accuracy of multidetector CT for the measurements of vertebral MPW in AIS has never been reported.

Volumetric acquisition allows further multiplanar reconstruction. Determining the coronal plane of the pedicle can be tricky, especially in curve summits where vertebrae are frequently asymmetric (7,9). Also, as small structures are concerned, it may be difficult to place the calliper on the inner cortical bone in a reproducible way. These two elements might involve small differences in measurements, which might be statistically significant considering the small size of the pedicle. These small sizes imply that the vast majority of the pedicle measurement underestimations were less than 1mm.

Screw diameter overestimation is a risk factor for medial, lateral, superior or inferior breaches, and then essentially for nerve injury. To our knowledge, in previously published

studies, authors have never considered such breaches of importance (i.e. producing symptoms and requiring screw removal) when they were less than 2mm (4,5,11,15–17). Considering the results of our study, spine surgeons might be tempted to raise MRI pedicle sizes by 10%. In light of these findings, and assuming that screw placement is otherwise optimal, there would be no reason to fear a significant breach since the overestimation of MPW is less than 1 mm. More significant breaches would be expected with oblique screw insertion, but this point is beyond the scope of our study: current optimal screw guidance relies on intra-operative imaging (CT, fluoroscopy or cone-beam CT), not pre-operative imaging (18–20).

A previous study reported thoracic pedicle width measurements with 2D MRI sequences but the authors did not validate these measurements with CT comparisons (25). Intra- and inter-reader ICC for CT measurements were consistent with previous studies (6). We could not compare our MR vs. CT ICCs with those of others as no previous study reported both MR and CT measurements in this pathological situation.

Our study has several limitations. One relates to the fact that pedicle length and orientation, two features of importance for spine surgeons (2,5), were not analyzed in our study. Our study population was small, but with 12 pedicles imaged per individual, the analysis was based on the measurement of 259 pedicles. Repeated measurements in given individuals might have introduced bias, but this was taken into account in our statistical analysis. Tomosynthesis may also be helpful, as this technique uses very low doses. Yet, this was not assessed in our study (26). Finally, we did not assess intraobserver reproducibility. One can assume that intraobserver reproducibility for CT and MRI is far from 100%, considering the small size of pedicles. Indeed this is rather intuitive in clinical practice, for example in oncology follow-ups, and this is particularly true when small structures are concerned. In our opinion, imperfect intraobserver reproducibility would stress the fact that the 10% difference identified may be clinically non-significant.

As a conclusion, although measures made with 3D T2-weighted spin echo sequences underestimate MPW by 10% compared to CT, we expect this difference would not increase the risk of pedicle breaches, provided screw placement is otherwise correct. 3D T2-weighted spin echo sequences are a valuable alternative to CT for preoperative measurements of vertebral pedicles in AIS patients. CT should no longer be used for this purpose. MRI should be preferred to CT because it is a non-radiating technique for adolescents suffering from AIS, without impairing procedure safety.

Conflicts of interest

The authors have no potential conflict of interest relevant to this article to disclose.

References

1. Dunn J, Henrikson NB, Morrison CC, Blasi PR, Nguyen M, Lin JS. Screening for adolescent idiopathic scoliosis: evidence report and systematic review for the US preventive services Task Force. *JAMA* 2018 ; 319:173–87.
2. Weinstein SL, Dolan LA, Cheng JCY, Danielsson A, Morcuende JA. Adolescent idiopathic scoliosis. *Lancet* 2008; 371:1527–37.
3. Akazawa T, Kotani T, Sakuma T, Minami S, Tsukamoto S, Ishige M. Evaluation of pedicle screw placement by pedicle channel grade in adolescent idiopathic scoliosis: should we challenge narrow pedicles? *J Orthop Sci* 2015; 20: 818–22.
4. Gautschi OP, Schatlo B, Schaller K, Tessitore E. Clinically relevant complications related to pedicle screw placement in thoracolumbar surgery and their management: a literature review of 35,630 pedicle screws. *Neurosurg Focus* 2011;31: 867-82.
5. Kwan MK, Chiu CK, Gani SMA, Wei CCY. Accuracy and safety of pedicle screw placement in adolescent idiopathic scoliosis patients: a review of 2020 screws using computed tomography assessment. *Spine* 2017;42:326–35.
6. Gao B, Gao W, Chen C, Wang Q, Lin S, Xu C, et al. What is the difference in morphologic features of the thoracic pedicle between patients with adolescent idiopathic scoliosis and healthy subjects? A CT-based case-control study. *Clin Orthop* 2017;475:2765–74.
7. Davis CM, Grant CA, Pearcy MJ, Askin GN, Labrom RD, Izatt MT, et al. Is there asymmetry between the concave and convex pedicles in adolescent idiopathic scoliosis? A cCT investigation. *Clin Orthop* 2017;475: 884–93.
8. Sarwahi V, Sugarman EP, Wollowick AL, Amaral TD, Lo Y, Thornhill B. Prevalence, distribution, and surgical relevance of abnormal pedicles in spines with adolescent

idiopathic scoliosis vs. No deformity: a CT-based study. *J Bone Joint Surg Am* 2014;96:92-118.

9. Brink RC, Schlösser TPC, Colo D, Vincken KL, van Stralen M, Hui SCN, et al. Asymmetry of the vertebral body and pedicles in the true transverse plane in adolescent idiopathic scoliosis: a CT-based study. *Spine Deform* 2017;5:37–45.
10. Cecen GS, Gulabi D, Cecen A, Oltulu İ, Guclu B. Computerized tomography imaging in adolescent idiopathic scoliosis: prone versus supine. *Eur Spine J* 2016;25:467–75.
11. Chan CYW, Kwan MK. Zonal differences in risk and pattern of pedicle screw perforations in adolescent idiopathic scoliosis (AIS): a computerized tomography (CT) review of 1986 screws. *Eur Spine J* 2018; 27: 340–9.
12. Murphy RF, Mooney JF. The crankshaft phenomenon. *J Am Acad Orthop Surg*. 2017;25: 185–93.
13. Yvert M, Diallo A, Bessou P, Rehel J-L, Lhomme E, Chateil J-F. Radiography of scoliosis: comparative dose levels and image quality between a dynamic flat-panel detector and a slot-scanning device (EOS system). *Diagn Interv Imaging* 2015;96:1177–88.
14. Ang EC, Robertson AF, Malara FA, O’Shea T, Roebert JK, Schneider ME, et al. Diagnostic accuracy of 3-T magnetic resonance imaging with 3D T1 VIBE versus computer tomography in pars stress fracture of the lumbar spine. *Skeletal Radiol* 2016;45: 1533–40.
15. Lavelle WF, Ranade A, Samdani AF, Gaughan JP, D’Andrea LP, Betz RR. Inter- and intra-observer reliability of measurement of pedicle screw breach assessed by postoperative CT scans. *Int J Spine Surg*. 2014;8:345-362.

16. Rao G, Brodke DS, Rondina M, Dailey AT. Comparison of computerized tomography and direct visualization in thoracic pedicle screw placement. *J Neurosurg* 2002; 97: 223–6.
17. Gertzbein SD, Robbins SE. Accuracy of pedicular screw placement in vivo. *Spine* 1990;15:11–4.
18. Macke JJ, Woo R, Varich L. Accuracy of robot-assisted pedicle screw placement for adolescent idiopathic scoliosis in the pediatric population. *J Robot Surg* 2016; 10:145–50.
19. Rajasekaran S, Bhushan M, Aiyer S, Kanna R, Shetty AP. Accuracy of pedicle screw insertion by AIRO® intraoperative CT in complex spinal deformity assessed by a new classification based on technical complexity of screw insertion. *Eur Spine J* 2018;9: 202-215.
20. Cordemans V, Kaminski L, Banse X, Francq BG, Cartiaux O. Accuracy of a new intraoperative cone beam CT imaging technique (Artis zeego II) compared to postoperative CT scan for assessment of pedicle screws placement and breaches detection. *Eur Spine J* 2017;26: 2906–16.
21. Andronikou S. Letting go of what we believe about radiation and the risk of cancer in children. *Pediatr Radiol* 2017;47:113–5.
22. Berrington de Gonzalez A, Salotti JA, McHugh K, Little MP, Harbron RW, Lee C, et al. Relationship between paediatric CT scans and subsequent risk of leukaemia and brain tumours: assessment of the impact of underlying conditions. *Br J Cancer* 2016;114: 388–94.
23. Doss M. Disavowing the ALARA concept in pediatric imaging. *Pediatr Radiol* 2017 ;47:118.

24. Leung RS. Radiation protection of the child from diagnostic imaging. *Curr Pediatr Rev* 2015; 11: 235–42.
25. Catan H, Buluç L, Anik Y, Ayyildiz E, Sarlak AY. Pedicle morphology of the thoracic spine in preadolescent idiopathic scoliosis: magnetic resonance supported analysis. *Eur Spine J* 2007:1203–8.
26. Blum A, Noël A, Regent D, Villani N, Gillet R, Gondim Teixeira P. Tomosynthesis in musculoskeletal pathology. *Diagn Interv Imaging* 2018;99:423–41.

Figure legends

Figure 1. Study flow chart.

Figure 2. 14-year-old girl with adolescent idiopathic scoliosis. A, B, CT reconstructions in the coronal plane of a right L3 pedicle, with minimal pedicle width measured by two different readers. Although the position of callipers seems correct on both images, minimal pedicle width measures differ by 7%.

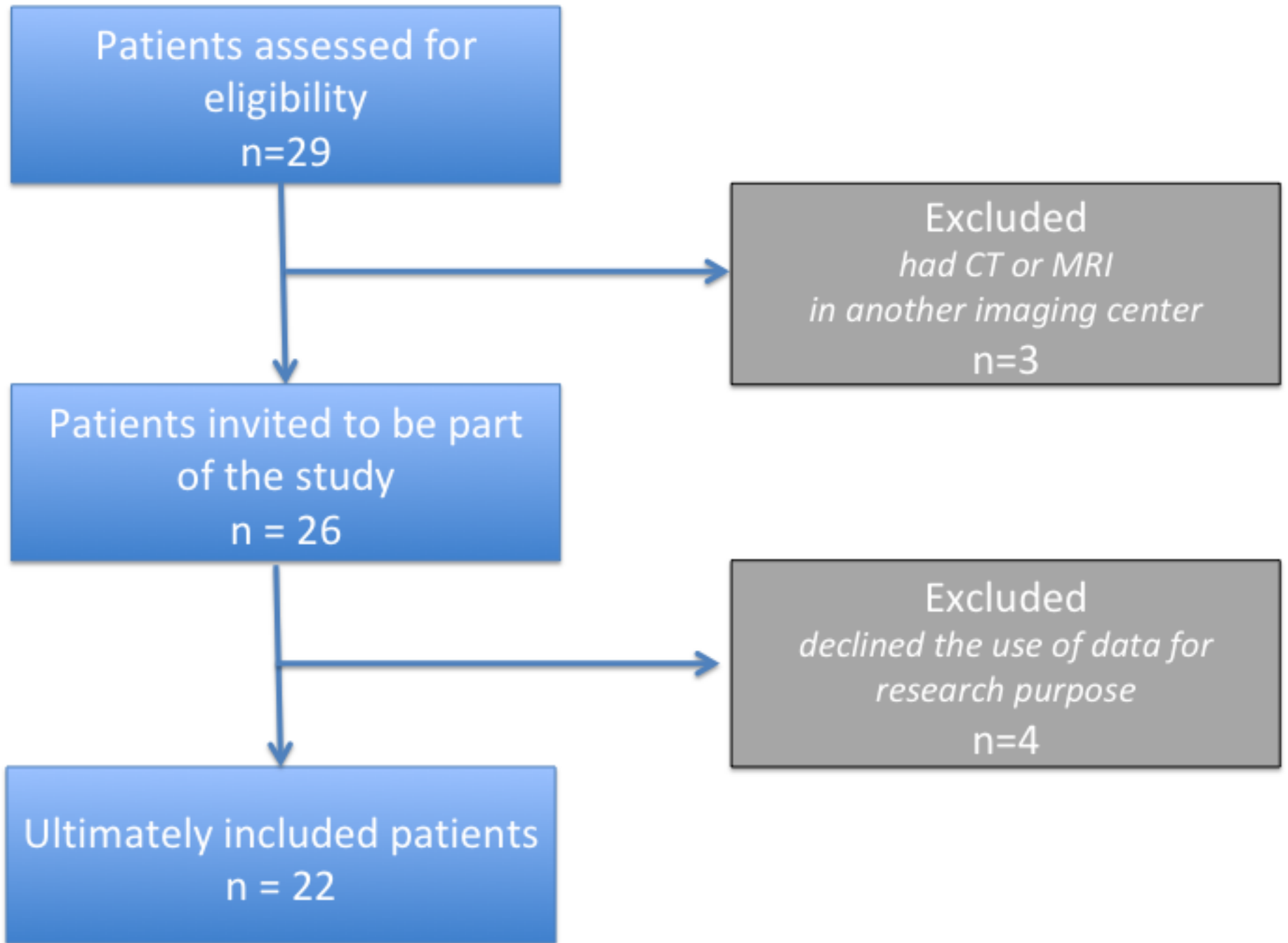
Figure 3. 14-year-old boy with adolescent idiopathic scoliosis and asymmetric L1 vertebra. A, Volume rendered image from CT data shows the L1 vertebra (arrow). B, C, D, Multiplanar reconstructions from 3D T2-weighted spin echo images, in the axial (B), sagittal (C), and coronal (C) planes show pedicles of the L1 vertebra. D, 3D T2-weighted image in the coronal plane shows minimal pedicle width measures. E, CT image in the coronal plane shows corresponding minimal pedicle width measures.

Figure 4. Boxplot shows distribution of relative differences for MRI-CT comparisons (blue boxes) and CT-CT comparisons (red boxes), depending on minimal pedicle width. Relative differences are expressed in percentages. Minimal pedicle widths are expressed in millimetres. Relative differences tend to increase for small pedicles although this was not statistically significant. The central rectangle goes from the first quartile (Q1) to the third quartile (Q3). Within the box, the bold horizontal lines represent the median. The dotted lines, called whiskers, extend from the bottom and top of the box. The bottom whisker goes from Q1 to the smallest non-outlier in the data set, and the top whisker goes from Q3 to the largest non-outlier. Individual outlying data points are displayed as unfilled circles.

Table 1. Parameters for three-dimensional T2-weighted spin-echo MRI.

Table 2. Distribution of minimal pedicle width measurements in 22 patients with adolescent idiopathic scoliosis.

Table 3. Intraclass correlation coefficients for CT-MRI agreement for both reader and inter-observer agreement for MRI and CT.





4,10 mm

L3 R

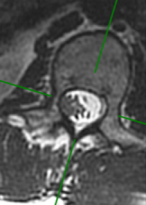


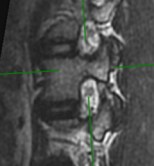
3,83 mm

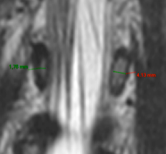
This is an axial MRI scan of the L3 vertebra. The image shows two vertebral bodies. The left vertebral body has a measurement line drawn across its width. The line is solid green from the center to the edge and dotted red from the edge to the edge. The text '3,83 mm' is written in red below the dotted portion of the line.

L3 R









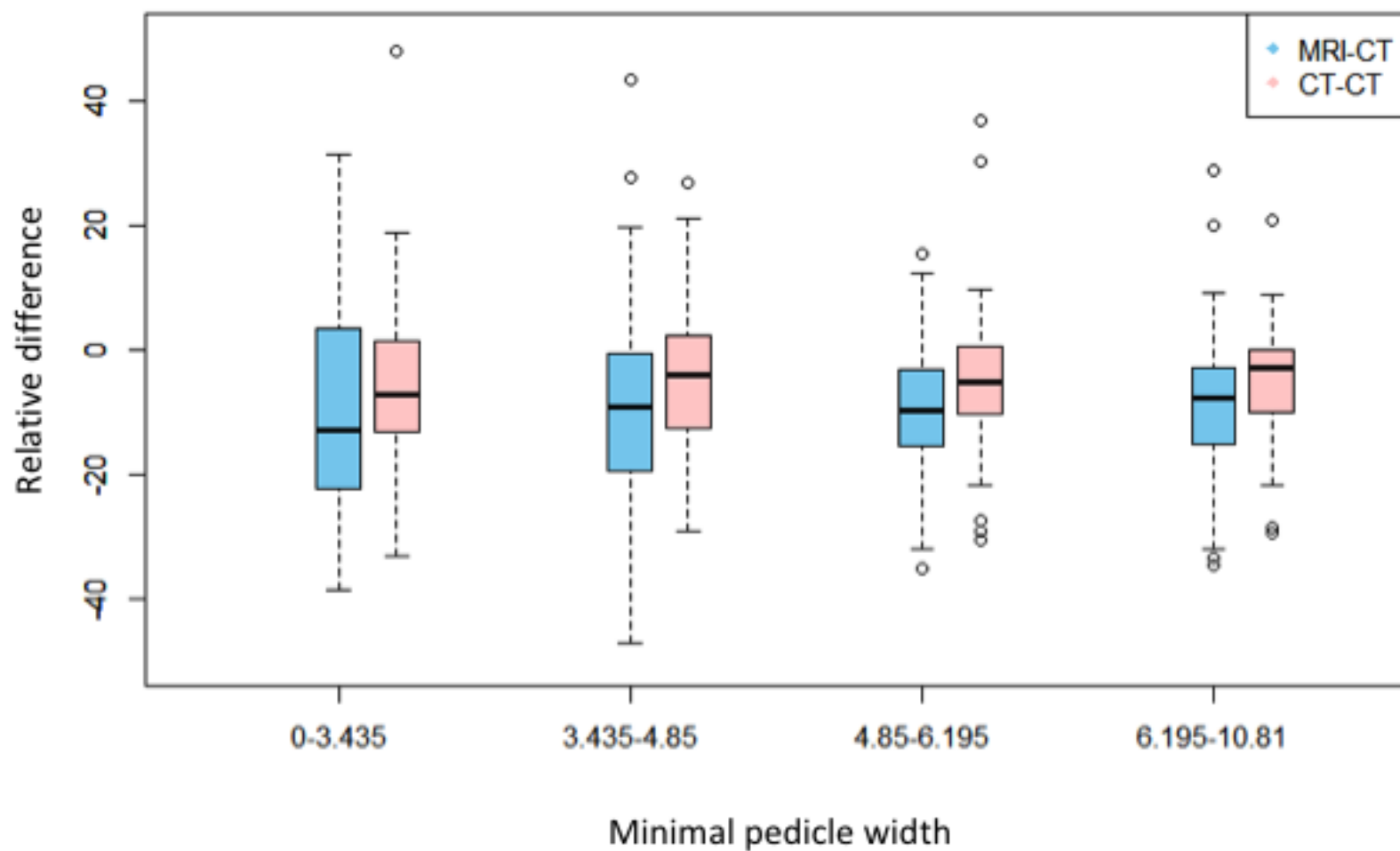
1,78 mm

4,13 mm

1,37 mm

4,18 mm





Parameter	Discovery® 750W	Discovery® 450W
Field strength (T)	3	1.5
Acquisition plane	Sagittal	Sagittal
Slice thickness (mm)	1	1
Field of view (mm ²)	350 × 245	350 × 245
Phase encoding direction	Antero-posterior	Antero-posterior
Matrix size	320 × 320	320 × 320
NEX	1	1
Reconstructed pixel size (mm ³)	0.6 × 0.6 × 0.6	0.6 × 0.6 × 0.6
TR (msec)	1400	1400
TE (msec)	60-139	80
Echo train length	100	92
Bandwith (Hertz)	83	83
Acquisition time	4 min 6 sec	4min 3 sec

Note. NEX = number of excitations; TR = time of repetition; TE = time of echo.

Pedicle	T12 R	T12 L	L1 R	L1 L	L2 R	L2 I	L3 R	L3 I	L4 R	L4 L	L5 R	L5 L	All pedicles
n	19	20	22	22	22	22	22	22	22	22	22	22	259
≤0.5	0 (0%)	0 (0%)	0 (0%)	1 (4.5%)	0 (0%)	0 (0%)	0 (0%)	0 (0%)	0 (0%)	0 (0%)	0 (0%)	0 (0%)	1 (0.4%)
]0.5; 1]	0 (0%)	0 (0%)	2 (9.1%)	0 (0%)	0 (0%)	0 (0%)	0 (0%)	0 (0%)	0 (0%)	0 (0%)	0 (0%)	0 (0%)	2 (0.8%)
]1; 0.5]	1 (5.3%)	0 (0%)	1 (4.5%)	1 (4.5%)	4 (18.2%)	2 (9.1%)	0 (0%)	0 (0%)	0 (0%)	0 (0%)	0 (0%)	0 (0%)	9 (3.5%)
]1.5; 2]	0 (0%)	0 (0%)	1 (4.5%)	3 (13.6%)	1 (4.5%)	2 (9.1%)	2 (9.1%)	0 (0%)	0 (0%)	0 (0%)	0 (0%)	0 (0%)	9 (3.5%)
]2; 2.5]	1 (5.3%)	1 (5%)	4 (18.2%)	0 (0%)	3 (13.6%)	3 (13.6%)	0 (0%)	0 (0%)	0 (0%)	0 (0%)	1 (4.5%)	0 (0%)	13 (5%)
]2.5; 3]	3 (15.8%)	2 (10%)	1 (4.5%)	3 (13.6%)	0 (0%)	3 (13.6%)	2 (9.1%)	2 (9.1%)	0 (0%)	0 (0%)	0 (0%)	0 (0%)	16 (6.2%)
]3; 3.5]	1 (5.3%)	1 (5%)	3 (13.6%)	1 (4.5%)	5 (22.7%)	0 (0%)	2 (9.1%)	3 (13.6%)	1 (4.5%)	0 (0%)	0 (0%)	1 (4.5%)	18 (6.9%)
]3.5; 4]	1 (5.3%)	1 (5%)	3 (13.6%)	2 (9.1%)	3 (13.6%)	1 (4.5%)	1 (4.5%)	1 (4.5%)	3 (13.6%)	3 (13.6%)	0 (0%)	1 (4.5%)	20 (7.7%)
]4; 4.5]	4 (21.1%)	1 (5%)	1 (4.5%)	2 (9.1%)	2 (9.1%)	4 (18.2%)	3 (13.6%)	1 (4.5%)	3 (13.6%)	0 (0%)	1 (4.5%)	0 (0%)	22 (8.5%)
]4.5; 5]	2 (10.5%)	2 (10%)	1 (4.5%)	3 (13.6%)	1 (4.5%)	2 (9.1%)	5 (22.7%)	3 (13.6%)	1 (4.5%)	5 (22.7%)	2 (9.1%)	1 (4.5%)	28 (10.8%)
]5; 5.5]	2 (10.5%)	6 (30%)	1 (4.5%)	2 (9.1%)	1 (4.5%)	2 (9.1%)	1 (4.5%)	2 (9.1%)	2 (9.1%)	1 (4.5%)	2 (9.1%)	3 (13.6%)	25 (9.7%)
]5.5; 6]	1 (5.3%)	2 (10%)	2 (9.1%)	2 (9.1%)	1 (4.5%)	1 (4.5%)	3 (13.6%)	3 (13.6%)	3 (13.6%)	3 (13.6%)	3 (13.6%)	1 (4.5%)	25 (9.7%)
]6; 6.5]	0 (0%)	1 (5%)	1 (4.5%)	0 (0%)	0 (0%)	1 (4.5%)	1 (4.5%)	2 (9.1%)	4 (18.2%)	3 (13.6%)	2 (9.1%)	2 (9.1%)	17 (6.6%)
]6.5; 7]	2 (10.5%)	1 (5%)	0 (0%)	1 (4.5%)	1 (4.5%)	0 (0%)	1 (4.5%)	1 (4.5%)	1 (4.5%)	0 (0%)	4 (18.2%)	4 (18.2%)	16 (6.2%)
]7; 7.5]	0 (0%)	0 (0%)	0 (0%)	0 (0%)	0 (0%)	0 (0%)	0 (0%)	2 (9.1%)	2 (9.1%)	2 (9.1%)	1 (4.5%)	2 (9.1%)	9 (3.5%)

]7.5; 8]	1 (5.3%)	0 (0%)	1 (4.5%)	0 (0%)	0 (0%)	1 (4.5%)	1 (4.5%)	0 (0%)	1 (4.5%)	3 (13.6%)	0 (0%)	1 (4.5%)	9 (3.5%)
]8; 8.5]	0 (0%)	1 (5%)	0 (0%)	0 (0%)	0 (0%)	0 (0%)	0 (0%)	0 (0%)	0 (0%)	2 (9.1%)	3 (13.6%)	0 (0%)	6 (2.3%)
]8.5; 9]	0 (0%)	1 (5%)	0 (0%)	1 (4.5%)	0 (0%)	0 (0%)	0 (0%)	1 (4.5%)	1 (4.5%)	0 (0%)	1 (4.5%)	1 (4.5%)	6 (2.3%)
]9; 9.5]	0 (0%)	0 (0%)	0 (0%)	0 (0%)	0 (0%)	0 (0%)	0 (0%)	1 (4.5%)	0 (0%)	0 (0%)	2 (9.1%)	2 (9.1%)	5 (1.9%)
]9.5; 10]	0 (0%)	0 (0%)	0 (0%)	0 (0%)	0 (0%)	0 (0%)	0 (0%)	0 (0%)	0 (0%)	0 (0%)	0 (0%)	1 (4.5%)	1 (0.4%)
]10; 10.5]	0 (0%)	0 (0%)	0 (0%)	0 (0%)	0 (0%)	0 (0%)	0 (0%)	0 (0%)	0 (0%)	0 (0%)	0 (0%)	1 (4.5%)	1 (0.4%)
]10.5; 11]	0 (0%)	0 (0%)	0 (0%)	0 (0%)	0 (0%)	0 (0%)	0 (0%)	0 (0%)	0 (0%)	0 (0%)	0 (0%)	1 (4.5%)	1 (0.4%)
Mean ± SD	4.3 ± 1.7	5.1 ± 1.7	3.5 ± 1.8	3.9 ± 2	3.3 ± 1.5	3.7 ± 1.7	4.5 ± 1.5	5.3 ± 1.8	5.6 ± 1.5	5.9 ± 1.5	6.5 ± 1.7	6.9 ± 2	4.9 ± 2
[range]*	[1.3 – 7.9]	[2.2 – 8.8]	[0.8 – 7.7]	[0 – 8.7]	[1.1 – 6.9]	[1.4 – 7.7]	[1.9 – 7.5]	[2.6 – 9.2]	[3.5 – 8.9]	[3.7 – 8.3]	[2 – 9.3]	[3.4 – 10.8]	[0 – 10.8]

Note. R: right; L: left. First column: size ranges (in mm). n corresponds to the number of pedicles. For each pedicle, the occurrence of size range is expressed as a number and a percentage (of total pedicles). The last column sums the occurrence of each size range. *Mean minimal width ± standard deviation (SD) and range of each pedicle.

Pedicle	CT reader 1 vs. MRI reader 1	CT reader 2 vs. MRI reader 2	MRI reader 1 vs. MRI reader 2	CT reader 1 vs. CT reader 2
T12-R	0.91 [0.67-0.97]	0.89 [0.68-0.96]	0.94 [0.87-0.98]	0.96 [0.84-0.99]
T12-L	0.87 [0.51-0.95]	0.88 [0.47-0.96]	0.97 [0.93-0.99]	0.95 [0.87-0.98]
L1-R	0.93 [0.69-0.98]	0.95 [0.85-0.98]	0.95 [0.88-0.98]	0.97 [0.85-0.99]
L1-L	0.92 [0.72-0.97]	0.95 [0.77-0.98]	0.98 [0.94-0.99]	0.98 [0.94-0.99]
L2-R	0.96 [0.89-0.98]	0.95 [0.87-0.98]	0.96 [0.9-0.99]	0.98 [0.94-0.99]
L2-L	0.94 [0.8-0.98]	0.91 [0.5-0.97]	0.96 [0.8-0.99]	0.98 [0.95-0.99]
L3-R	0.92 [0.65-0.97]	0.93 [0.78-0.97]	0.96 [0.89-0.98]	0.93 [0.84-0.97]
L3-L	0.91 [0.66-0.97]	0.88 [0.61-0.95]	0.91 [0.77-0.96]	0.96 [0.84-0.99]
L4-R	0.81 [0.36-0.93]	0.87 [0.59-0.95]	0.93 [0.84-0.97]	0.91 [0.77-0.97]
L4-L	0.86 [0.58-0.95]	0.84 [0.66-0.93]	0.8 [0.59-0.91]	0.85 [0.5-0.94]
L5-R	0.76 [0.5-0.89]	0.84 [0.61-0.93]	0.9 [0.77-0.96]	0.9 [0.78-0.96]
L5-L	0.89 [0.54-0.96]	0.86 [0.7-0.94]	0.95 [0.89-0.98]	0.92 [0.79-0.97]

Note. L = left side; R = right side; ICC = intra-class correlation coefficient; 95%CI = 95% confidence interval; CT = computed tomography; MRI = magnetic resonance imaging; Numbers in brackets are 95%CI.